




Unraveling the True Atomic Structures of Exotic Oxides

*Thomas Proffen and Takeshi Egami**

High-temperature superconductors (HTSCs) and certain oxides with unusual magnetic properties, such as LiNiO_2 , are promising technological materials. But to understand their electronic or magnetic properties, one must know how these materials are constructed at the atomic and slightly larger length scales. A new technique for analyzing neutron-diffraction data—coupled with the high-quality data provided by LANSCE's high-resolution neutron powder diffractometer—has led to the discovery of totally unexpected nanoscale domains in LiNiO_2 and to an apparent confirmation of the presence of nanoscale structural inhomogeneities in HTSC cuprates. These inhomogeneities could play a key role in high-temperature superconductivity.

** University of Tennessee*



In 1912, Bragg discovered a law relating a crystal's structure to the diffraction pattern produced when the crystal is illuminated by x-rays. Since then, scientists have been able to determine the atomic structures of increasingly complex materials. Diffraction patterns produced by illuminating crystalline powders with x-rays or neutrons, called powder diffraction, have been a large part of that revolution in materials science, and the data analysis technique for powder diffraction data known as full profile refinement, or Rietveld analysis, is now routine. This technique reveals many features of the structure including lattice parameters, atomic positions, or atomic displacement parameters. However, Rietveld analysis determines only the average long-range structure of the material, because only the intensities and positions of the diffraction pattern's peaks—the “Bragg” peaks—are analyzed. The simple example shown in Figure 1 reveals the limitations of Rietveld analysis.

Figure 1a shows two artificial, two-dimensional structures that have one atomic site per unit cell, and identical site occupancies of 30 and 70 percent for atoms of type A (in light blue) and B (in purple), respectively. (The site occupancy for a given type of atom is the fraction of the atomic sites occupied in the lattice by that atom type.) The only difference between the two structures is the atomic ordering. Whereas the two types of atoms in the right lattice are randomly distributed, the arrangement of atoms in the left lattice exhibits “chemical” short-range order: The A atoms are clustered together. Figure 1b shows the powder-diffraction patterns generated by computer simulation for these two artificial lattices. Rietveld analysis of the two patterns yields identical results for both structures because the intensities and positions of the Bragg peaks are the same. This is no sur-

prise, since the “average” structures of both lattices are the same. Rietveld analysis cannot distinguish between the two structures, and this article would end here if we could not obtain additional information from the diffraction data.

In fact, the difference between the two structures is clear in the diffuse-scattering signal shown in the inset of Figure 1b. This signal, which consists of the comparatively small intensity fluctuations between the Bragg peaks, contains information about the chemical short-range order that is revealed in the structures' pair distribution functions (PDFs), shown in Figure 1c. A PDF is simply the Fourier transform of the total-scattering pattern, which includes both Bragg and diffuse scattering. The chemical short-range order is apparent in the difference between the two PDFs shown in Figure 1c. However, diffuse scattering can reveal not only chemical short-range order but also any deviation from the average structure of a sample. In fact, the PDF method was originally used to study glasses and liquids, which have no long-range order.

The Pair Distribution Function

The PDF gives the probability of finding an atom at a distance r from another atom. In other words, the (primary) information contained in the PDF is the distribution of the bond lengths between all the atoms in a sample. Because it is obtained from the total-scattering pattern, the PDF contains structural information over a range of length scales. In fact, the ability to provide structural information at different length scales is one of the PDF's great strengths.

For example, consider the C_{60} molecules (“buckyballs”) shown in Figure 2. A single buckyball is shown

in Figure 2a. Buckyballs can form crystals with long-range order, as shown in Figure 2b. At room temperature, the individual balls within the crystal rotate (nearly) freely with respect to each other. The plot of total-scattering data shown in Figure 2c was used to obtain the PDF results plotted in Figure 2d. The PDF results reflect the rotation of each of the buckyballs. The C-C pairs within each molecule produce sharp peaks in the PDF for distances smaller than the buckyball diameter (~ 0.7 nanometers). The PDF is broad and nearly featureless at larger distances because there are only weak correlations between the molecules. For a detailed summary of these results, see Takeshi Egami and Simon Billinge (2003).

The Neutron Powder Diffractometer (NPDF)

Because the PDF is the Fourier transform of the scattering data, the PDF's resolution is determined by the maximum momentum transfer Q of the measurement. In most cases, a synchrotron source providing high-energy x-rays or a spallation neutron source such as that at LANSCE is used to perform experiments that will be analyzed with PDFs. The advantages of using neutrons over x-rays are discussed elsewhere in this issue. Neutrons are the probe of choice for samples containing light elements (e.g., hydrogen or lithium) or samples with adjacent elements in the periodic table, for example nickel and copper. The only instrument dedicated to studying disordered materials with the neutron PDF technique is the NPDF at LANSCE's Lujan Neutron Scattering Center (Figure 3). The diffractometer's large range of Q values enables one to detect local structural distortions of ~ 0.01 nanometer, and its high Q values provide usable PDF data for atom-atom distances of more

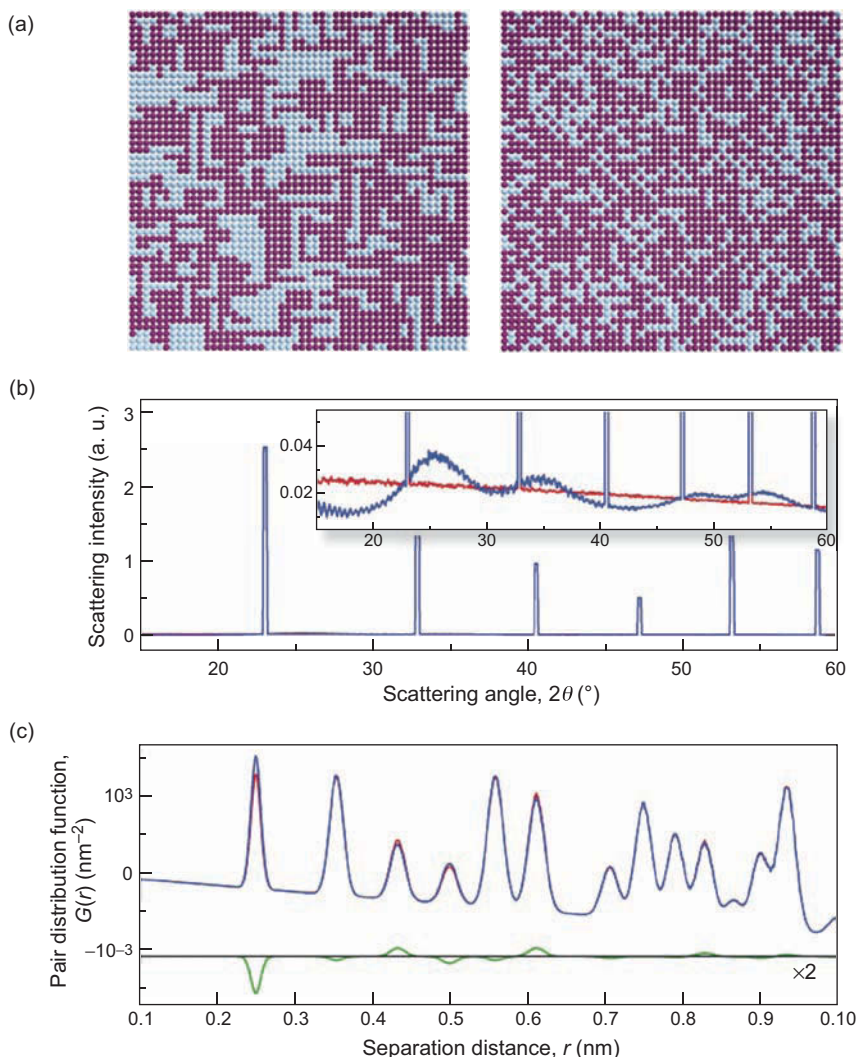


Figure 1. Understanding the Information Contained in Diffraction Data
 (a) These panels show two artificial, two-dimensional lattices. Each consists of 50×50 atomic sites, with one atomic site per unit cell. Each site is occupied by an A atom (light blue) or a B atom (purple). The site occupancies for the A and B atoms are the same for both lattices. The site occupancy for a given type of atom is the fraction of the atomic sites occupied by that atom type in a lattice. In this case, the site occupancies for the A and B atoms are 30% and 70%, respectively. The structures differ in the short-range ordering of the A atoms. In the left lattice, the A atoms are clustered together; in the right lattice, they are distributed randomly. (b) This panel shows powder diffraction patterns for the two structures. The intensities and positions of the Bragg peaks are identical in both cases because Bragg scattering reveals only the average long-range structure of the material, which in this case is determined by the site occupancies of the A and B atoms. However, the diffuse scattering in the inset clearly shows the difference between the two structures. The blue curve is for the lattice on the left; the red curve is for the lattice on the right. (c) The PDFs in the bottom panel were obtained from the total-scattering data, that is, data for both Bragg and diffuse scattering. The PDFs contain information about the short-range structural ordering, as shown in the differences between the two PDFs. The difference between the two curves, enlarged by a factor of 2, is also shown in this panel (green curve).

than 20 nanometers. A typical measurement with the NPDF takes 3 to 8 hours, depending on sample size.

The NPDF is available for experiments through the User Program at the Lujan Neutron Scattering Center. Applications for beam time are accepted twice a year or through fast-access proposals at the LANSCE webpage (<http://www.lansce.lanl.gov>). Below we discuss some exciting results from recent experiments performed with the NPDF.

Example I: Nickelate with Nanoscale Domains

Although lithium nickelate has a simple chemical formula, LiNiO_2 , the compound's behavior is complex and mysterious. Lithium nickelate consists of layers of Li^+ ions sandwiched between slabs of NiO_2 (see Figure 4). When lithium is deficient (that is, there are vacancies at some of the crystal's lithium sites), lithium ions can move within the lattice, making the compound a fast ionic conductor. But LiNiO_2 's magnetic properties are intriguing as well because the Ni^{3+} ions form triangular networks in the NiO_2 slabs. For those interested in special magnetic order, a triangular network of ions with magnetic moments, or spin, is like a bone to a dog—an ideal playmate. That is so because spin ordering can be frustrated, or blocked from occurring, if the exchange interaction between spins is negative.

In spin ordering, the ions' magnetic spins adjust their orientations to lower the compound's total magnetic energy. Any mechanism or property that prevents this lowering is said to “frustrate” the magnetic ordering. Let us assume that the individual spins of three Ni^{3+} ions form a triangle and are connected through a negative exchange interaction. Here, a negative exchange interaction means that the

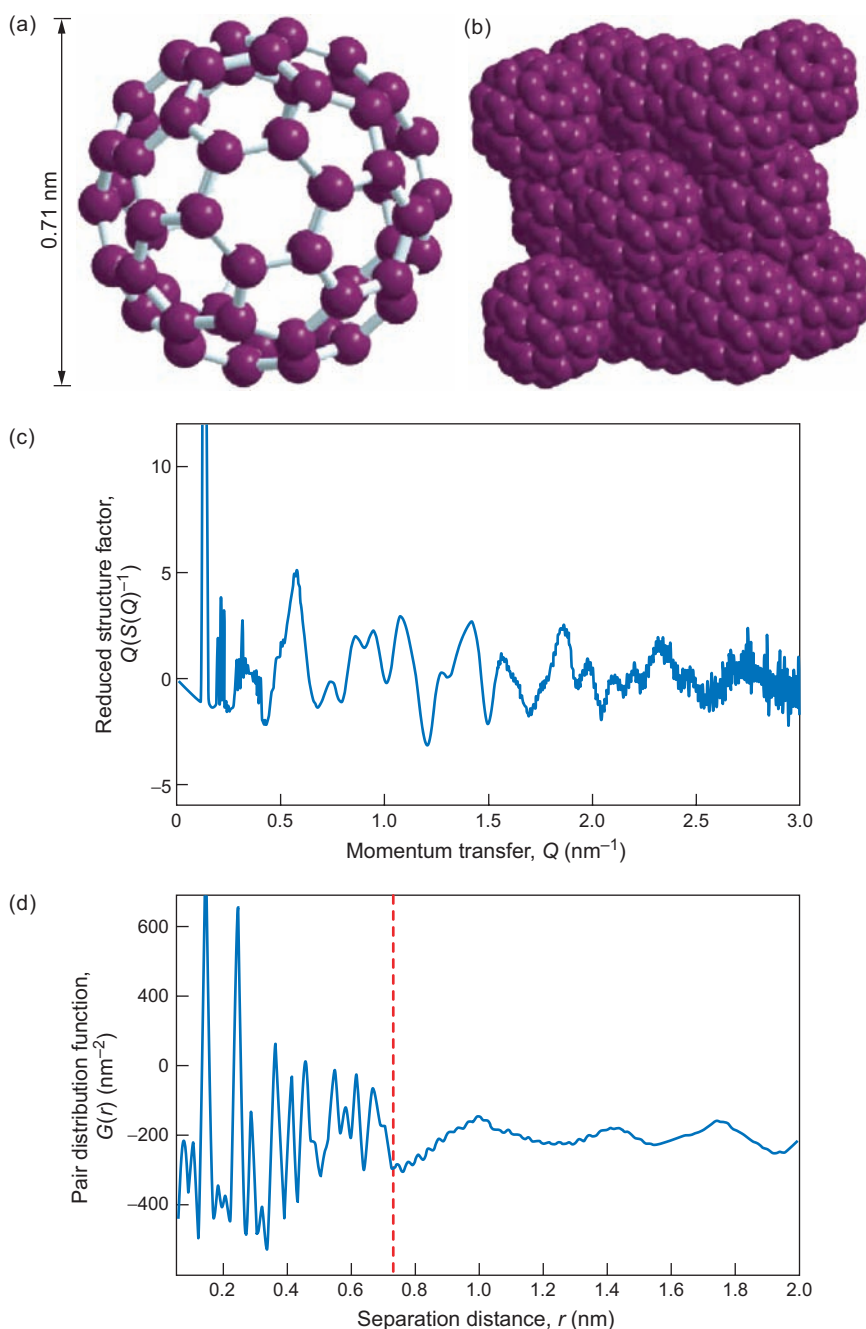


Figure 2. Buckyball Crystals

Buckyballs, or molecules of C_{60} , shown in (a) can form crystals with long-range order (b). We Fourier-transformed the normalized neutron-scattering intensity of a C_{60} crystal (c) to obtain the PDF (d). The PDF shows sharp peaks for distances smaller than the diameter of a single C_{60} molecule; the diameter is indicated by the red vertical dashed line. These peaks correspond to the C–C distances within a single buckyball. For larger distances, there are no sharp peaks, indicating that, at room temperature, there are almost no correlations between C atoms in different C_{60} molecules. [The data are from Egami and Billinge (2003).]

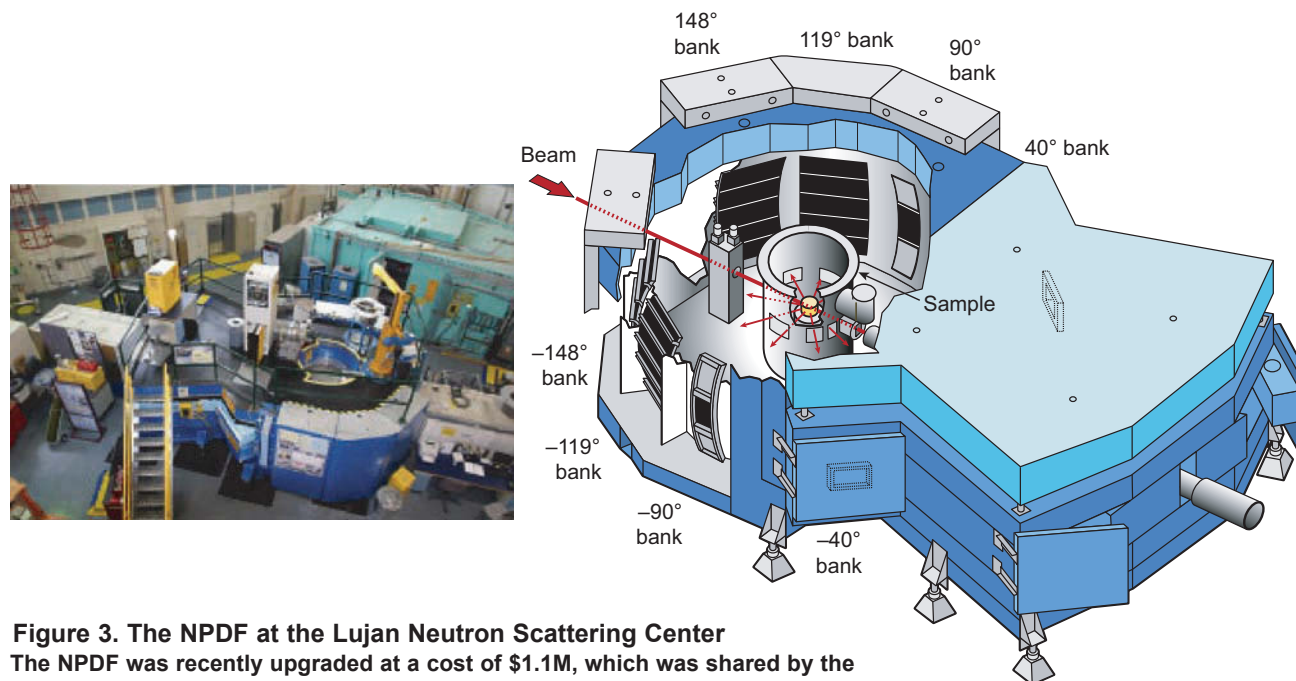


Figure 3. The NPDF at the Lujan Neutron Scattering Center
The NPDF was recently upgraded at a cost of \$1.1M, which was shared by the National Science Foundation, several academic institutions, and Los Alamos National Laboratory. Now among the world's leading diffractometers, the NPDF is dedicated to studies of the atomic structure of complex materials.

preferred, or lowest-energy, state (the ground state) of the compound should be an antiferromagnetic spin configuration—one in which neighboring spins are antiparallel. However, if we let two of the triangle's spins be antiparallel, as shown in Figure 5, then the third spin would not know which way to point, and the transition to an antiferromagnetic state would be frustrated. Philip W. Anderson suggested (1973) that the quantum-mechanical ground state of such a system could be the resonating valence bond (RVB) state made of dynamic spin-singlet (or antiparallel-spin) pairs. The RVB state shows no phase transition to antiferromagnetic order. Indeed, LiNiO_2 shows no magnetic transition, even though Ni^{3+} clearly has a nonzero spin, $S = \frac{1}{2}$. But there is no credible confirmation of the RVB state in LiNiO_2 . The true spin ground state of this compound remains a mystery.

The ordering of the electronic orbitals of the Ni^{3+} ions seems to

be frustrated as well. A Ni^{3+} ion is a so-called Jahn-Teller (JT) ion. Such ions prefer the local atomic environment to be distorted in order to minimize the electronic energy. Each Ni^{3+} ion is surrounded by six oxygen ions, forming a NiO_6 octahedron. Ni^{3+} has seven d-electrons. Six of these electrons fill the three orbitals designated as t_{2g} , so that their total angular and spin momenta are zero, which is to say that their spatial distribution is spherically symmetric (that is, it has no preferred direction). The last d-electron goes into one of the two orbitals designated as e_g , which have z^2 and $x^2 - y^2$ symmetry, respectively. In a lithium nickelate crystal with cubic symmetry, the two orbital states would have the same energy and would therefore be called "degenerate." But if the O_6 octahedron becomes distorted, the degeneracy is lifted, and the energy level of one state decreases, and that of the other is raised. (As the degeneracy is

lifted, the original states also become new states.) In this distorted environment, the seventh electron takes on the lower energy state. Indeed, in the crystal of a sister compound, NaNiO_2 , the NiO_6 octahedra are JT distorted, and the collective JT distortion across the crystal causes it to distort macroscopically. However, there is no hint of crystal distortion in LiNiO_2 . Hence, it has been argued that the orbital ordering of the e_g state in LiNiO_2 is also frustrated, and therefore LiNiO_2 forms an "orbital" glass state (Chung et al. 2005) in which the d-electrons in the e_g orbitals have no long-range order; that is, they are randomly oriented.

The results we have obtained with the NPDF suggest a different arrangement state (Chung et al. 2005) as shown in Figure 6. To perform our experiments, we loaded a powder of LiNiO_2 in a vanadium can (vanadium is "transparent" for neutrons and often used as container material for neutron

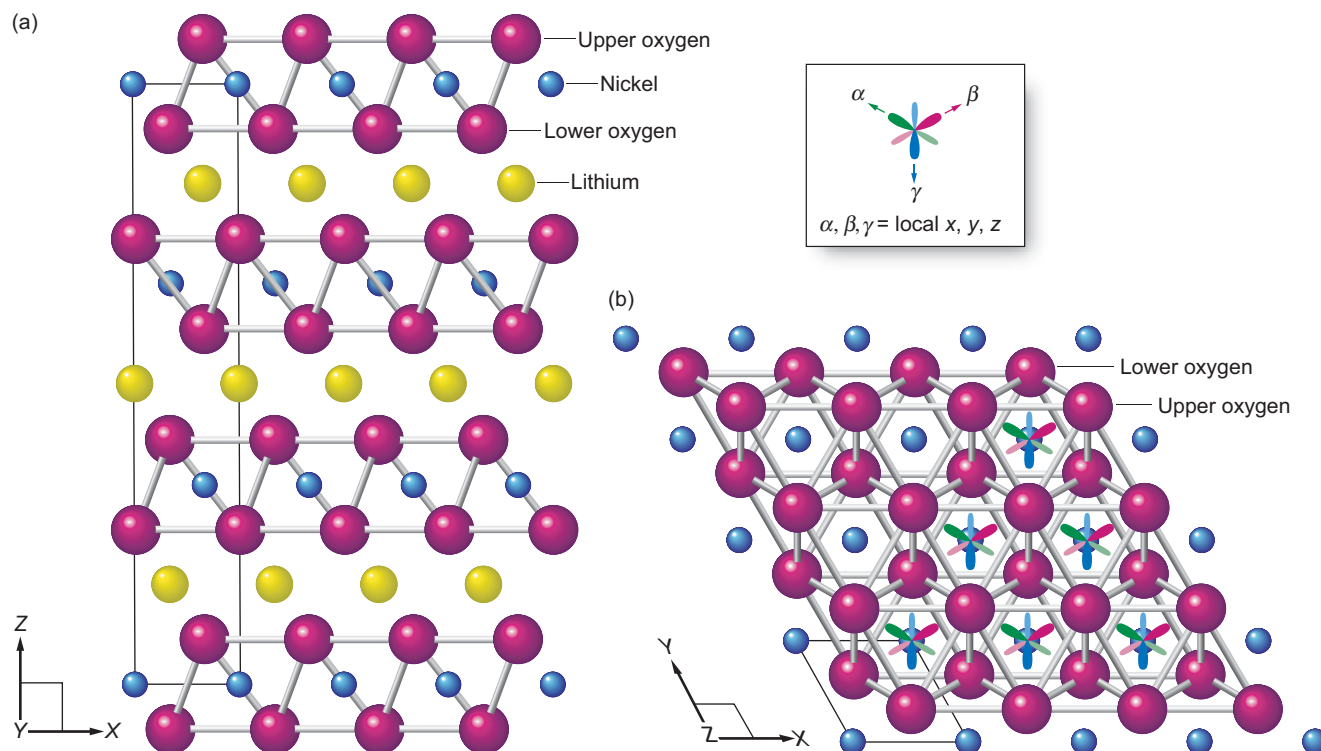


Figure 4. The Crystal Structure of Lithium Nickelate (LiNiO_2)

LiNiO_2 consists of layers of Li^+ ions sandwiched between slabs of NiO_2 . (a) This side view of LiNiO_2 shows that the thin solid lines connecting four nickel sites define the boundary of a unit cell. (b) The Ni^{3+} ions form a triangular network within each NiO_2 slab, making for an interesting magnetic ordering of the compound, as discussed in the text and shown in Figure 5. Each Ni^{3+} ion has seven d-electrons, six of which form spherically symmetrical orbitals. The orbital of the seventh d-electron can point in one of three orthogonal directions, shown as α , β , and γ . The collinear, double-lobed structures represent the possible orientations of the seventh d-electron. Using the PDF method to analyze NPDF data taken on LiNiO_2 , we have determined the local ordering of the seventh d-electron orbitals to be as shown in Figure 7.

diffraction) and measured the powder diffraction at various temperatures. We then Fourier-transformed the scattering results to obtain the PDFs. As mentioned, the NPDF's high resolution allows us to determine the PDF for separation distances of up to 20 nanometers, which is a factor of 4 higher than results obtained elsewhere so far—refer to Figure 6a. From the PDF, we see that the nearest-neighbor environment of Ni^{3+} (out to 0.25 nanometer) is indeed JT distorted. Notice the shoulder on the blue curve

on the high- r side of the first PDF peak in Figure 6b. That shoulder represents the longer Ni–O bond and indicates the JT distortion. However, by modeling the medium-range order (between approximately 0.5 and 2 nanometers), we found that the local JT distortions are not collinear but point in three directions perpendicular, or “orthogonal,” to each other (refer to Figure 7). Below about 375 kelvins, the local JT distortions form three sublattices corresponding to the three directions. Because the local distur-

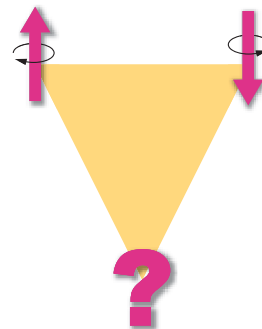


Figure 5. Frustrated Magnetic-Spin Ordering

This drawing shows how an antiferromagnetic system with a magnetic spin at each vertex of a triangle cannot lower its magnetic energy by orienting the neighboring spins so that they are antiparallel. This drawing applies to the magnetic spins of the Ni^{3+} ions in LiNiO_2 , which form a triangular network, as shown in Figure 4.

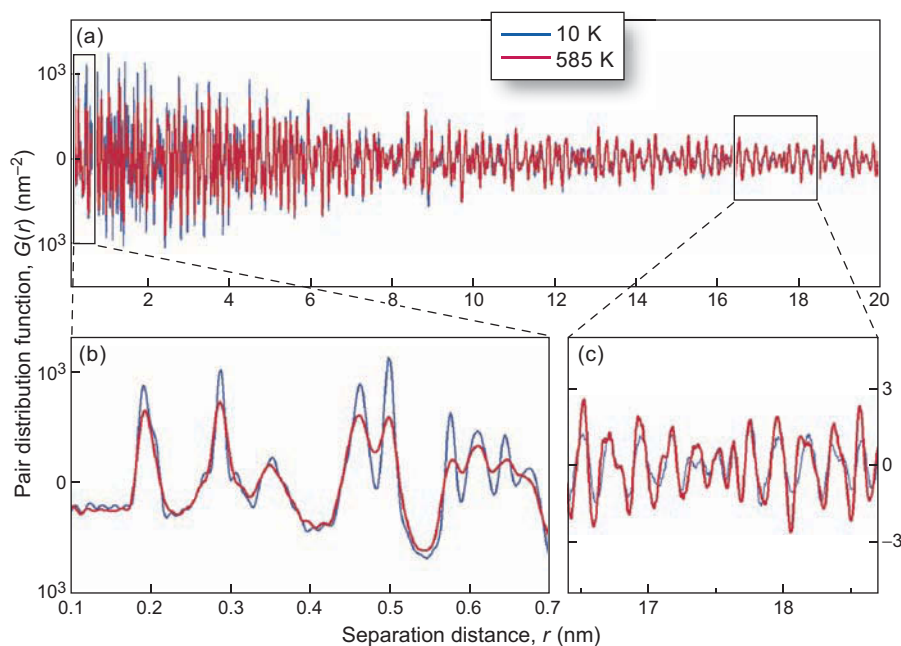


Figure 6. PDFs of LiNiO_2

These plots are from data of LiNiO_2 taken with the NPDF at 10 K (blue curves) and 585 K (red curves). (a) The full range of the data is shown for atom-atom separation distances of up to 20 nm. (b) In the low- r (near-neighbor) region, the PDF peaks broaden as the temperature increases. (c) In the high- r (far-neighbor) region, the opposite occurs, providing direct evidence for the existence of nanoscale domains, which decrease the crystal's long-range order.

tions are orthogonal, there is no macroscopic distortion.

The PDF results also surprised us in another respect. Because the PDF measures atomic correlations, its peaks usually become sharper at low temperatures as thermal vibrations diminish. Indeed, the peaks at short distances for LiNiO_2 's PDFs do exactly that. However, the peaks at distances larger than 8 or 9 nanometers actually become broader at lower temperatures—refer to Figure 6c. This feature is observed because the local JT distortions are orthogonal, so that the inversion symmetry of the NiO_2 plane is lost, and the plane wants to curve. [In a lattice with inversion symmetry, an atom present at point (x, y, z) has a corresponding atom present at point $(-x, -y, -z)$.]

The result is that domains about 10 nanometers in size form below 375 kelvins. The orbital ordering of the three sublattices is preserved within a domain, and the curvature reverses at a domain boundary (Chung et al. 2005). The formation of the nanodomains frustrates the long-range ordering of the orbital orientations.

Our PDF analysis of NPDF data has furthered our understanding of LiNiO_2 's atomic structure, as well as of its electronic structure through the JT distortion, and may help us understand anomalous experimental observations of the compound's magnetic spin susceptibility. Understanding the material's magnetic interactions could in turn help us develop new technological materials.

Example II: Possible Electronic Inhomogeneity in Superconducting Cuprates

Cuprates that exhibit high-temperature superconductivity (HTSC) are another example of intriguing oxides with local complexity. When the HTSC phenomenon was discovered in 1986 (Bednorz and Müller), many theorists predicted it would be understood fairly quickly because they claimed to already know, more or less, what was going on—although they could not agree on exactly which theory was right. History has since shown how wrong they were and how complex the phenomenon is.

One of the most intriguing complexities of the high-temperature cuprate superconductors is the pronounced inhomogeneity of their electronic structure. This inhomogeneity is baffling, since electronic disorder will scatter and break the Cooper pairs, which are the charge carriers that produce superconductivity. On the other hand, there are many superconductors whose structures are strongly disordered. For instance, some amorphous metallic alloys, such as niobium-boron (Nb-B), are superconducting. But the length scale of the structural disorder (atomic scale) for Nb-B is quite different from its superconducting coherence length (tens or hundreds of nanometers). By contrast, the superconducting coherence length of high-temperature cuprate superconductors is only a few nanometers, and these cuprates appear to have structural inhomogeneities with a similar length scale. The presence of these structural inhomogeneities was first suggested by indirect measurements (Egami and Billinge 1996), although most workers in the field dismissed the inhomogeneities as merely “dirt” (that is, unwanted impurities introduced during sample making) irrelevant to HTSC, or as byproducts of strong coupling at best. Recently,

however, several beautiful images of nanoscale structural inhomogeneities, which were obtained by scanning tunneling microscopy (STM), have appeared in the literature (Pan et al. 2001, Lang et al. 2002, McElroy et al. 2003). It has therefore become more difficult to ignore the possibility that structural inhomogeneities could be an integral part of HTSC. And yet, because STM is a surface probe, the inhomogeneity observed by STM may be considered a surface phenomenon.

To investigate the possibility that structural inhomogeneities are integral to HTSC, we examined a series of high-temperature cuprate superconductors, namely, $\text{La}_{2-x}\text{Sr}_x\text{CuO}_4$ (LSCO), with the NPDF. The parent compound, $x = 0$, is a charge transfer insulator (Zaanen 1985) with long-range antiferromagnetic order. Replacing La^{3+} with Sr^{2+} dopes, or introduces holes into, the system, and these cuprates show HTSC for $0.06 \leq x \leq \sim 0.25$. We obtained PDFs of powdered LSCO samples with x varying from 0 to 0.3. Figure 8 shows the PDFs at $T = 10$ kelvins as functions of distance r and composition x . These PDFs show that the long-range structure (larger than 2 nanometers) varies smoothly with x , while there are anomalous structural variations at distances smaller than 2 nanometers. In particular, deviations from the average structure, as determined by Rietveld analysis, are stronger below 2 nanometers. Although we are still analyzing the details, the results obtained with the NPDF thus far appear to be consistent with those of the STM studies and to indicate that the inhomogeneities exist within the volumes of the materials, not just at their surfaces. At present, however, we do not know what kind of structural deviations exist in these samples. It will be interesting to see how accurately data obtained with the NPDF and analyzed by the PDF technique allow determining the real structures of these strange

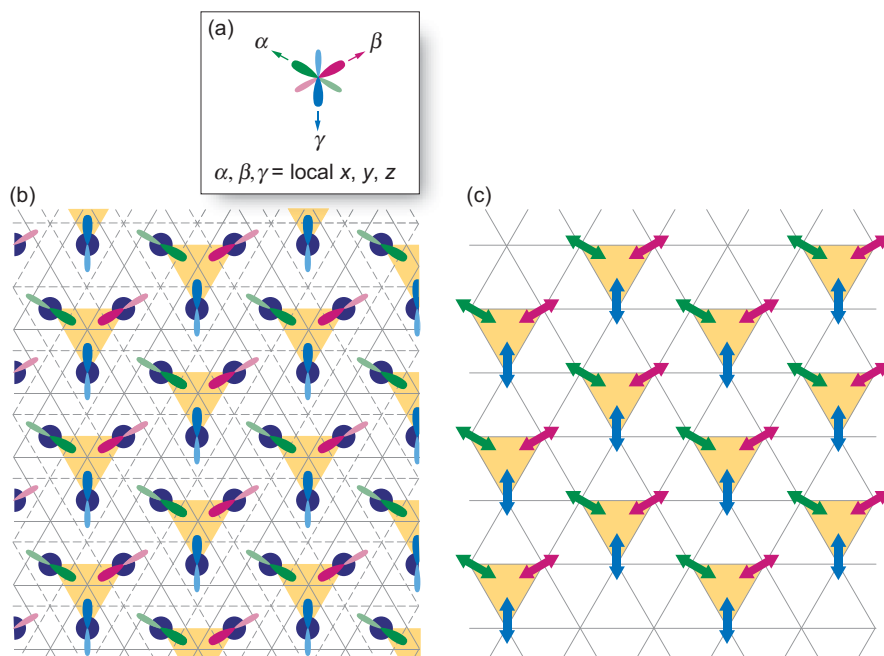


Figure 7. PDF Results for Local Orbital Ordering

(a) A three-dimensional perspective is shown of the three possible orientations of the seventh d-electron orbitals for a single Ni^{3+} ion. (b) Illustrated here is the local ordering of the seventh d-electron orbitals of the Ni^{3+} ions in LiNiO_2 . The dark blue circles are the Ni^{3+} ions. The solid and dashed lines are the upper and lower oxygen planes, respectively (see also Figure 4). We deduced this ordering by comparing PDFs obtained from NPDF measurements of LiNiO_2 with the PDFs of several models of the orbitals' possible orientations. Our analysis shows that this ordering extends over nanoscale domains with sizes of ~ 10 nm. (c) The double-headed arrows indicate the three possible orientations of the orbitals in a particular domain and correspond to three different sublattices (each sublattice corresponds to a differently colored double-headed arrow). In fact, the orbitals for the three sublattices are not in a single plane but are orthogonal, which is why the crystal is not macroscopically distorted—unlike LiNiO_2 's sister compound, NaNiO_2 . In (b) and (c), the orbitals appear to be in a single plane because of the top-view perspective.

and complex cuprates.

We also studied $\text{Na}_{0.3}\text{CoO}_2 \cdot 1.4\text{H}_2\text{O}$, another strange oxide superconductor, a cobaltate that incorporates water molecules in its structure. This cobaltate has the same structure as LiNiO_2 except for the intercalated water (Takada et al. 2003). For our neutron-diffraction studies of this cobaltate, we replaced hydrogen with deuterium to better see the locations of the water molecules. Results indicate that the

water molecules are strongly modified in this compound, but further analysis is needed to understand the implications of this new finding.

It is likely that such nanoscale, multilevel complexities are not uncommon in complex oxides. No doubt, in the future, there will be many opportunities for using the PDF technique on NPDF data to help solve the structural mysteries of other interesting compounds. ■

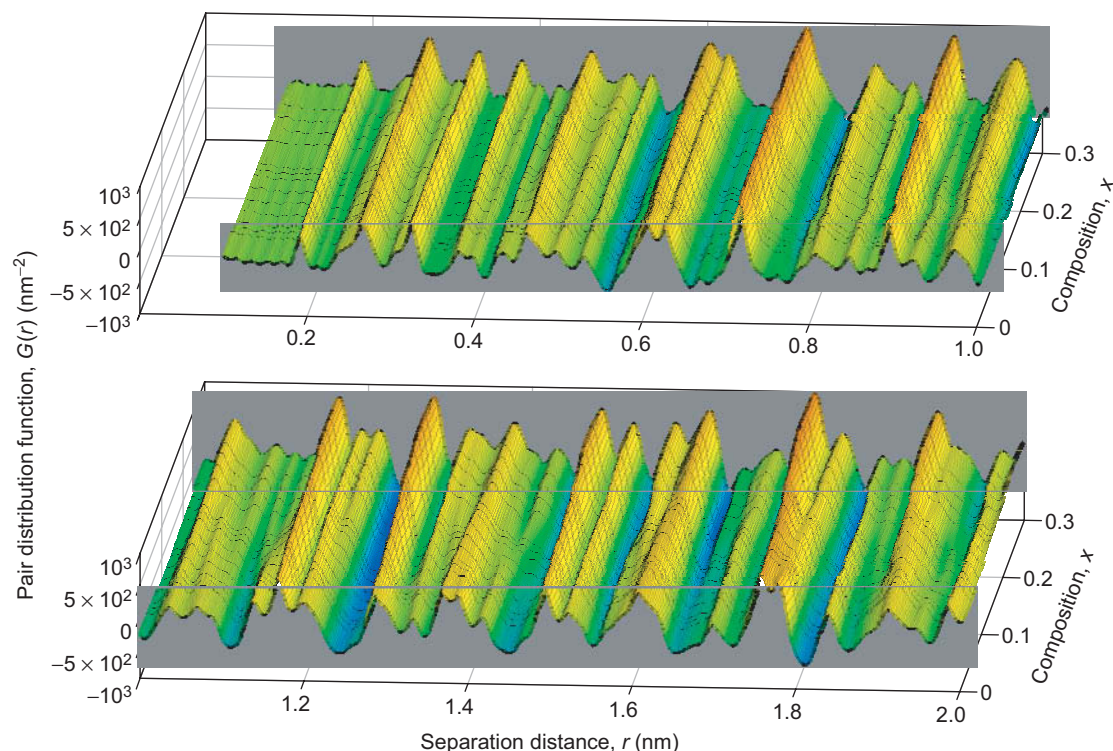


Figure 8. PDFs of $\text{La}_{2-x}\text{Sr}_x\text{CuO}_4$, a High-Temperature Superconductor, as a Function of Composition x
 All data were taken at $T = 10$ K. Rietveld analysis of the total scattering data suggests that the long-range structure varies smoothly with composition, but these PDF results clearly show structural inhomogeneities to a separation distance of 2 nm. Although some studies had provided similar results, these are the first systematic studies revealing such inhomogeneities, which could be an integral part of high-temperature superconductivity.

Further Reading

- Anderson, P. W. 1973. Resonating Valence Bonds: A New Kind of Insulator? *Mater. Res. Bull.* **8**: 153.
- Bednorz, J. G., and K. A. Müller. 1986. Possible High T_c Superconductivity in the Ba-La-Cu-O System. *Z. Phys. B* **64**: 189.
- Chung, J.-H., Th. Proffen, S. Shamoto, A. M. Ghorayeb, L. Croguennec, W. Tian et al. 2005. Local Structure of LiNiO_2 Studied by Neutron Diffraction. *Phys. Rev. B* **71**: 064410.
- Egami, T., and S. J. L. Billinge. 1996. Lattice Effects in High- T_c Superconductors. In *Physical Properties of High Temperature Superconductors V*. Edited by D. M. Ginsberg. River Edge, NJ: World Scientific.
- . 2003. *Underneath the Bragg Peaks: Structural Analysis of Complex Materials*. Amsterdam: Pergamon.
- Lang, K. M., V. Madhavan, J. E. Hoffman, E. W. Hudson, H. Eisaki, S. Uchida, and J. C. Davis. 2002. Imaging the Granular Structure of High- T_c Superconductivity in Underdoped $\text{Bi}_2\text{Sr}_2\text{CaCu}_2\text{O}_{8+x}$. *Nature* **415**: 412.
- McElroy, K., R. W. Simmonds, J. E. Hoffman, D. H. Lee, J. Orenstein, H. Eisaki et al. 2003. Relating Atomic-Scale Electronic Phenomena to Wave-Like Quasiparticle States in Superconducting $\text{Bi}_2\text{Sr}_2\text{CaCu}_2\text{O}_{8+x}$. *Nature* **422**: 592.
- Pan, S. H., J. P. O'Neal, R. L. Badzey, C. Chamon, H. Ding, J. R. Engelbrecht et al. 2001. Microscopic Electronic Inhomogeneity in the High- T_c Superconductor $\text{Bi}_2\text{Sr}_2\text{CaCu}_2\text{O}_{8+x}$. *Nature* **413**: 282.
- Takada, K., H. Sakurai, E. Takayama-Muromachi, F. Izumi, R. A. Dilanian, and T. Sasaki. 2003. Superconductivity in Two-Dimensional CoO_2 Layers. *Nature* **422**: 53.
- Zaanen, J., G. A. Sawatzky, and J. W. Allen. 1985. Band Gaps and Electronic Structure of Transition-Metal Compounds. *Phys. Rev. Lett.* **55** (4): 418.